Chapter 17

Piezoelectric Cantilever Biosensors for Label-free, Real-time Detection of DNA and RNA

Alexander P. Haring, Ellen Cesewski, and Blake N. Johnson

Abstract

This chapter reviews the design, fabrication, characterization, and application of piezoelectric-excited millimeter-sized cantilever (PEMC) sensors. The sensor transduction mechanism, sensing principle, and mode of operation are discussed. Bio-recognition strategies and surface functionalization methods for detection of DNA and RNA are discussed with a focus on self-assembly-based approaches. Methods for the verification of biosensor response via secondary binding assays, reversible binding assays, and the integration of complementary transduction mechanisms are presented. Sensing applications for medical diagnostics, food safety, and environmental monitoring are provided. PEMC sensor technology provides a robust platform for the real-time, label-free detection of DNA and RNA in complex matrices over nanomolar (nM) to attomolar (aM) concentration ranges.

Key words Biosensor, Biosensing, Piezoelectric, Cantilever, Bio-recognition, Resonant mode, Dynamic mode, Resonant frequency, Real-time detection, Resonant frequency shift

1 Introduction

1.1 Background on Cantilever-Based DNA and RNA Sensing

The quantification of DNA and RNA has many applications in medical diagnostics, food safety, and environmental monitoring [1–6]. To date, sensor-based approaches to DNA and RNA quantification have emerged as potential complements to traditional methods-based assays, such as polymerase chain reaction (PCR), given their ability to sensitively detect DNA and RNA in real-time via label-free protocols [5, 7, 8]. Specifically, dynamic-mode cantilever sensors have provided sensitive detection of synthetic and biologically derived DNA and RNA in complex matrices over wide dynamic ranges [7].

A class of dynamic-mode cantilever sensors, known as piezoelectric-excited millimeter-sized cantilever (PEMC) sensors, has provided sensitive detection of DNA and RNA in complex matrices, including body fluids, [9] food matrices, [10] and source

Ben Prickril and Avraham Rasooly (eds.), *Biosensors and Biodetection: Methods and Protocols, Volume 2: Electrochemical, Bioelectronic, Piezoelectric, Cellular and Molecular Biosensors*, Methods in Molecular Biology, vol. 1572,
DOI 10.1007/978-1-4939-6911-1_17,

water [11]. DNA and RNA target strands as short as 10–30 bases [9, 12] as well as relatively longer strands of sheared nuclear DNA and ribosomal RNA have been detected. [10, 11] For example, PEMC sensors have been shown to provide sample preparation-free detection of miRNA biomarkers [9] and genetic markers of food- and water-borne pathogens [10, 11]. It has also been shown that target strands which contain a single nucleotide polymorphism (SNP) exhibit a reduced sensor response relative to fully complementary target strands, [9] which suggests a promising future for sensor-based approaches to SNP identification.

1.2 Sensing Principle

As shown in Fig. 1a, b, PEMC sensors transduce the binding between an immobilized probe and a target species into a measureable shift in the resonant frequency of the self-sensing and -exciting piezoelectric layer. The resonant frequency of the cantilever sensor is given by: [7, 13, 14]

$$f_n = \frac{1}{2\pi}\left(\frac{\lambda_n}{L}\right)^2 \sqrt{\frac{EI}{\rho_c wt}} \tag{1}$$

where f_n is the resonant frequency of the nth mode, λ_n is the nth root of $1 + cos(\lambda_n)cosh(\lambda_n) = 0$, L is the cantilever length, w is the cantilever width, t is the cantilever thickness, E is the Young's modulus, I is the moment of inertia for a cantilever, and ρ_c is the cantilever density. The first three eigenvalues are: $\lambda_1 \sim 1.875$, $\lambda_2 \sim 4.694$, and $\lambda_3 \sim 7.855$ [15, 16]. Since the sensor mass (m_c) is related to geometry and material properties through the relationship $m_c = \rho_c Lwt$, the resonant frequency may also be expressed as:

$$f_n = \frac{{\lambda_n}^2}{2\pi}\sqrt{\frac{EI}{L^3 m_c}} \tag{2}$$

Assuming the effective stiffness of the cantilever $(k) = EI/L^3$, the resonant frequency takes the form:

$$f_n = \frac{{\lambda_n}^2}{2\pi}\sqrt{\frac{k}{m_c}} \tag{3}$$

Thus, an increase in the sensor mass caused by the hybridization of a target DNA or RNA strand to an immobilized DNA probe will result in a decrease in the resonant frequency. The effect of mode order (n) on the dynamic sensor mass is given as: [15]

$$f_n = \frac{1}{2\pi}\sqrt{\frac{k}{\left({}^{m_c}/_{\lambda^4}\right)}} \tag{4}$$

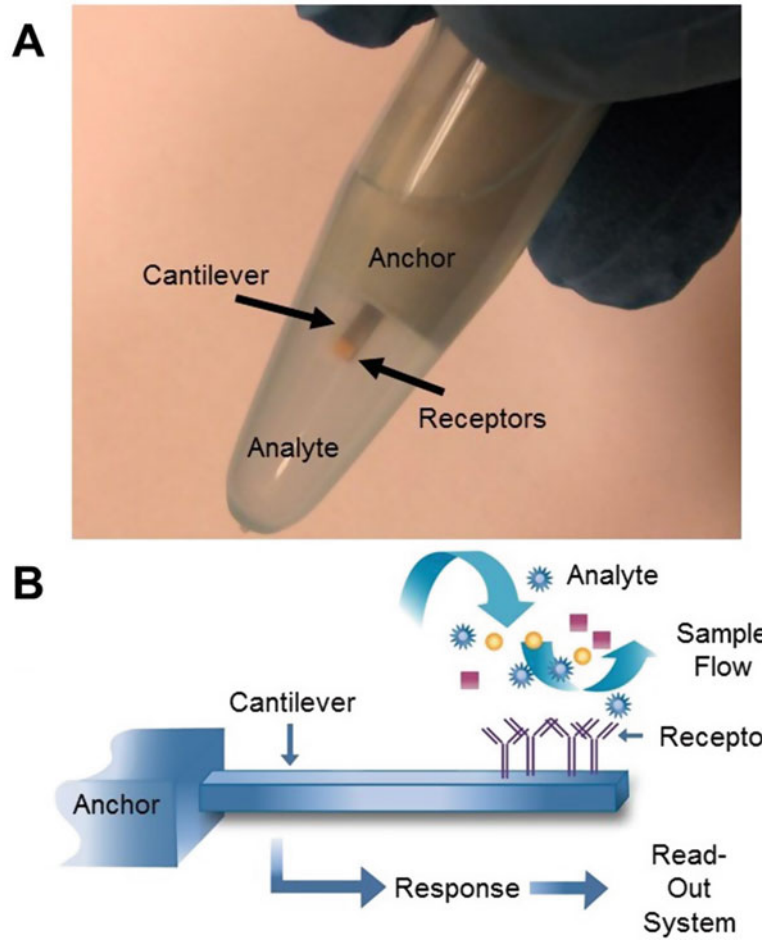

Fig. 1 (**a**) Photograph of a piezoelectric-excited millimeter-sized cantilever (PEMC) sensor immersed in a liquid sample in a static flow setting (unpublished data). (**b**) Schematic of the dynamic-mode cantilever sensing principle by which the specific binding of target species, such as DNA or RNA strands, to immobilized probes, such as single-stranded DNA, is transduced via a change in the sensor resonant frequency. Adapted from Johnson and Mutharasan with permission from Elsevier [7]

Equation (4) may then be used to estimate the resonant frequency shift (Δf) for a given mass change (Δm) as: [7, 17]

$$\frac{\Delta f}{f_n} = -\frac{1}{2}\frac{\Delta m}{m_{c,n}} \tag{5}$$

where $m_{c,n}=m_c/\lambda_n^4$ is the effective sensor mass. Given PEMC sensors are millimeter scale (L=2–4 mm) and produce high frequency resonant modes (f=30 kHz–1 MHz), they are capable of sustaining resonance while immersed in viscous liquid environments [13]. The effect of the cantilever geometry and operation frequency on

damping characteristics may be characterized by the magnitude of the cantilever Reynolds number (Re_c): [18]

$$Re_c = \frac{\rho_f \omega w^2}{4\mu} \tag{6}$$

where ρ_f and μ are the density and viscosity of the fluid, respectively, and ω is the characteristic radial frequency of vibration ($=2\pi f_n$). In the limit of $Re_c \to \infty$ the fluid is considered to be inviscid in nature [18]. Thus, as shown in Fig. 2a, b, PEMC sensors enable the real-

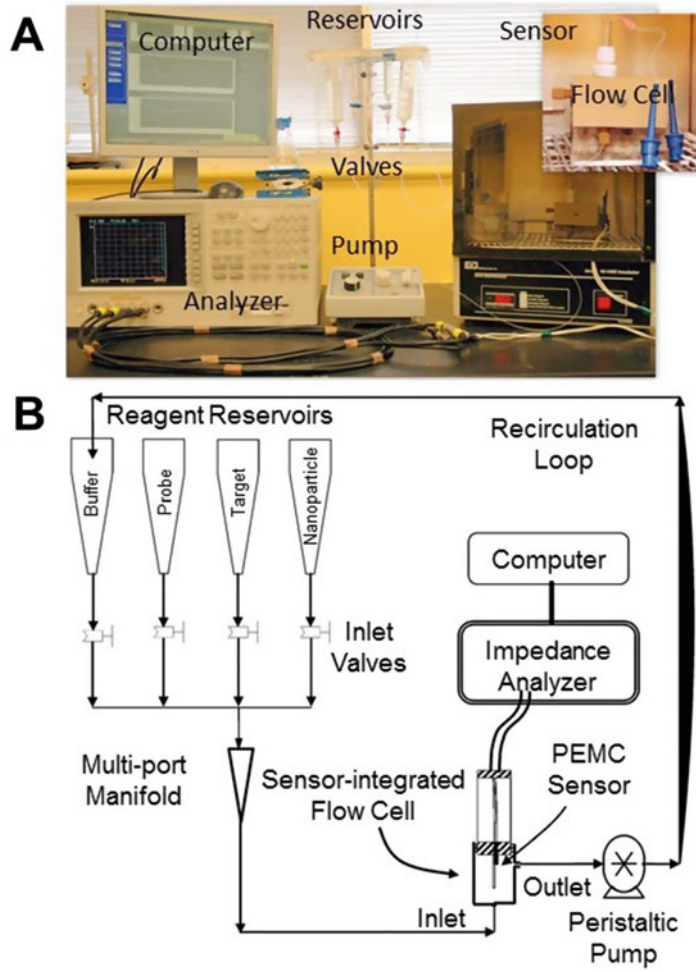

Fig. 2 (**a**) Photograph of the experimental apparatus showing the primary components which include an impedance analyzer, PEMC sensor, flow cell, incubator, and pump. Adapted from Johnson and Mutharasan with permission from the American Institute of Physics [22]. (**b**) Schematic of the fluid handling system and flow loop diagrams used for real-time biosensing. Adapted from Johnson and Mutharasan with permission from the American Institute of Physics [22]

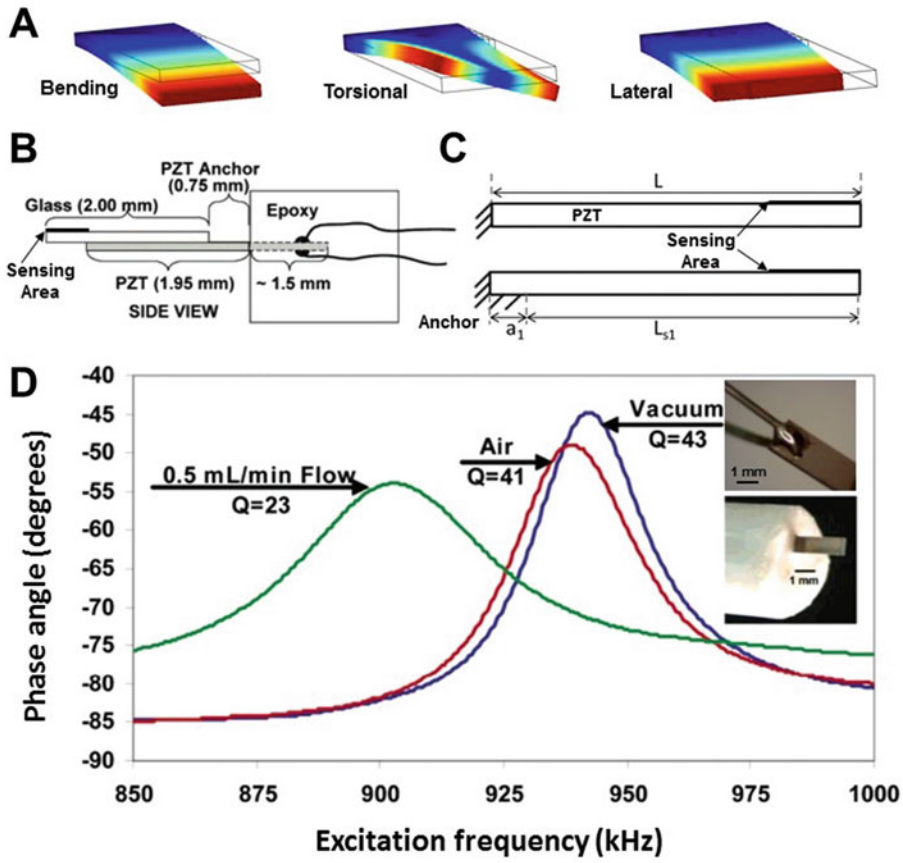

Fig. 3 (**a**) Cantilever mode shapes for bending, torsional, and lateral modes (red color indicates region of high total displacement; blue color indicates region of low total displacement). Schematic of PEMC sensor composite and single layer designs (**b** and **c**, respectively). Reproduced from Maraldo et al. with permission from the American Chemical Society [33] and Sharma et al. with permission from Elsevier [21]. (**d**) Sensor impedance spectra in vacuum (f~945 kHz, Q-value=43), air (f~940 kHz, Q-value=41), and water (f~900 kHz, Q-value=23). *Top inset* shows a representative solder bond used to connect the PZT chip with conductive wires. Bottom inset shows the associated PEMC sensor used in the impedance measurement. Reproduced from Maraldo et al. with permission from the American Chemical Society [33]

time detection of DNA and RNA in continuously flowing liquid. We note that PEMC sensors give rise to various resonant mode shapes depending on the excitation frequency (*see* Fig. 3a), which have been shown to be sensitive to molecular binding; [19, 20] however, the majority of applications have used the bending mode as it is typically the fundamental mode.

1.3 Method Overview

The application of PEMC sensors for detection of DNA and RNA involves four primary steps of: (1) fabrication, (2) surface functionalization, (3) sensing studies, and (4) sensor response verification. Sensor fabrication steps include material assembly, anchoring, and electrical insulation. Surface functionalization procedures involve

surface preparation, bio-conjugation, bio-recognition, and surface passivation strategies. Sensing studies encompass exposure of the target-containing sample to the sensor and the continuous real-time monitoring of sensor response. Sensor response verification procedures include reversible binding assays, secondary binding assays, the integration of complementary transduction mechanisms, and the use of reference sensors.

2 Materials

2.1 Sensor Components

1. Lead zirconate titanate (PZT) (Type 5A, Piezo Systems, Inc., Woburn, MA, USA).
2. Solder kit (Nickel (Ni), Piezo Systems, Inc., Woburn, MA, USA).
3. Epoxy (Loctite 1C–LV Hysol).
4. Cyanoacrylate (Loctite 430).
5. Glass tubes (Inner diameter=6 mm).
6. Conductive wire (30 gauge).
7. Micro-soldering iron.
8. Solder (Rosin core, Kester).

2.2 Electrical Insulation

1. Polyurethane.
2. Parylene C.
3. Spin coater (Radius=16 cm, Dynamic II Centrifuge, Clay Adams).
4. Chemical vapor deposition system (PDS 2010 Labcoter 2, SCS).

2.3 Fluid Handling System and Supporting Instrumentation

1. Reagent vessels (Syringes, Male Luer-Lok™, 5, 10, and 50 mL, BD).
2. Inlet valves (Stopcock with Luer connections, 1-Way, Male lock, Cole Parmer).
3. Multi-port manifold.
4. Tubing (Outer diameter=1/16 in., Polyethylene tubing, Warner Instruments).
5. Microfluidic fittings (Flangeless ferrule, 1/16 in. outer diameter tubing, Upchurch Scientific; Flangeless male nut, 1/16 in. outer diameter tubing, Polyetheretherketone (PEEK), Upchurch Scientific).
6. Sensor flow cell (PEEK).
7. Peristaltic pump (Variable flow mini-pump, Cole Parmer).
8. Impedance analyzer (HP4294A, Agilent).
9. Computer.

2.4 Surface Preparation

1. Plasma treatment, argon (Ar).
2. Plasma reactor (PDC-001, Harrick Plasma).

2.5 Bio-conjugation

1. Gold (Au) target.
2. Sputtering system (DESK IV, Denton Vacuum, Inc., Moorestown, NJ, USA).
3. Piranha solution, concentrated sulfuric acid (H_2SO_4) and hydrogen peroxide (30% v/v, H_2O_2), 3:1 v/v H_2SO_4:H_2O_2.

2.6 Bio-recognition

1. Thiolated single-stranded DNA probe (Integrated DNA Technologies, Coralville, IA, USA).
2. Nuclease-free deionized water (DIW).
3. Sodium chloride (NaCl).
4. Tris(2-carboxyethyl)phosphine (TCEP).
5. Tris-hydrochloride (Tris–HCl).
6. Ethylenediaminetetraacetic acid (EDTA).
7. Tris-EDTA (TE) buffer, 1×, 10 mM Tris–HCl in DIW, 1 mM EDTA in DIW, pH=7.9, 1 M NaCl.

2.7 Surface Passivation

1. 1-mercapto-6-hexanol (MCH).
2. Ethanol (EtOH), 200 proof.
3. TE buffer, 1×.

2.8 Target Hybridization

1. Single-stranded DNA or RNA target (synthetic or derived from cellular extract).

2.9 Secondary Hybridization

1. Gold nanoparticles (AuNPs) (Diameter=15 nm, BBInternational, Cardiff, UK).
2. Secondary thiolated single-stranded DNA probe (Integrated DNA Technologies, Coralville, IA, USA).

2.10 Reversible Binding

1. Sodium hydroxide (NaOH), 0.75 M in DIW.

3 Methods

The methods are organized into four primary categories: (1) fabrication, (2) surface functionalization, (3) sensing studies, and (4) sensor response verification. Sensor fabrication involves material assembly, anchoring, and electrical insulation. Surface functionalization involves surface preparation, DNA probe immobilization, and surface passivation. Sensing studies encompass target preparation, target exposure, and continuous sensor monitoring. Sensor

response verification includes reversible binding assays for sensor regeneration in the form of target dehybridization and secondary binding assays for sensor amplification in the form of DNA-functionalized AuNP hybridization.

3.1 Sensor Assembly

1. The 127 μm thick PZT sheet with Ni electrodes is diced into 5×1 mm^2 chips (American Dicing, Liverpool, NY, USA).
2. As shown schematically in Fig. 3b, conductive wires are then micro-soldered to both faces of the PZT chip, forming a cantilever (*see* **Note 1**). The solder bond is positioned ~ 0.5 mm from the back edge of the PZT chip. Typical solder bonding areas are 0.1–0.2 mm^2. Excessive soldering temperatures are avoided to prevent damage to the PZT layer. A representative micrograph of the solder bond is provided in Fig. 3d.
3. The solder joint and chip are then embedded within an epoxy-filled 6 mm glass tube leaving 2–4 mm of the PZT layer extending beyond the epoxy anchor, thus maintaining a cantilever geometry.
4. To actuate sensitive impedance-coupled modes, a second passive layer, such as borosilicate glass, is often bonded to the active PZT layer, for example using cyanoacrylate (*see* Fig. 3b) [20]. We note that the bonding layer has been omitted from Fig. 3b, but exists at the interface between the active PZT layer and the passive layer. Alternatively, sensitive resonant modes may be actuated in single layer cantilevers by extending the epoxy anchor on one side of the cantilever, typically 0.2–1 mm, as shown schematically in Fig. 3c, while the other side remains at the original free length [21]. Actuation strategies based on asymmetric electrode configurations have also been used [22].

3.2 Electrical Insulation

1. A polyurethane layer is first spin-coated onto all cantilever faces and edges at a speed of ~ 1.5 krpm for 30 s, and is allowed to cure overnight.
2. The polyurethane spin-coated PEMC sensors are then coated with a 10 μm thick layer of Parylene C via chemical vapor deposition (*see* **Note 2**).
3. As shown representatively in Fig. 3d, after the sensor is electrically insulated, the impedance spectrum is then examined in different environments, such as vacuum, air, and water. The resonant frequency decreases with increasing density of the surrounding medium, which is an expected result for dynamic-mode cantilevers [23]. We note that the typical variation of sensor impedance characteristics, such as resonant frequency and Q-value, for a batch of similarly fabricated sensors is $\sim 5\%$ ($n = 3$ sensors) [9].

3.3 Surface Preparation

1. Prior to the deposition of a thin Au film, which provides sites for chemisorption of thiolated DNA probes, the sensor is rinsed with EtOH.
2. The sensor is then cleaned using a 5 min, single cycle, Ar plasma treatment.

3.4 Bio-conjugation

1. The sensor is masked except for a 1 mm^2 region at the cantilever tip which is reserved as the selective sensing area (*see* Fig. 3b, c).
2. For immobilizing DNA probes through Au-thiolate chemistry, a 100 nm Au layer is sputtered onto the exposed area of the cantilever tip.
3. To ensure efficient immobilization of thiol molecules, the flow cell and reagent reservoirs are rinsed with EtOH and DIW. The Au surface is cleaned by treatment with piranha solution for ~ 30 s. The sensor is then rinsed with DIW (*see* **Note 3**).

3.5 Bio-recognition

1. As shown in Fig. 4a, the detection of a DNA or RNA target requires the initial immobilization of a DNA strand, commonly called a DNA probe, which is complementary to a region of the target strand, typically 10–20 bases in length. The thiolated DNA probe is supplied by the vendor in disulfide form. The disulfide bond is reduced by adding 1 μL of TCEP to 300 μL of 3 μM probe solution, mixing, and allowing the mixture to react for 60 min at room temperature. The stock solution is then used to create serial dilutions in buffer ranging from nanomolar (nM) to femtomolar (fM) levels (*see* **Notes 4** and **5**).
2. The experimental setup consists of an impedance analyzer, a peristaltic pump, a custom flow cell, and several fluid reservoirs. The flow cell is machined to contain one cylindrical chamber to hold the sensor anchor and a second cylindrical chamber extension (120 μL reactor volume) to house the PEMC sensor. The flow cell is kept in an incubator to maintain isothermal conditions. The flow loop is operated in either a single pass or recirculation mode.
3. Prior to an experiment, the flow cell and loop are rinsed with EtOH followed by DIW.
4. The sensor resonant frequency is continuously monitored by a custom LabView program. The algorithm for the LabView program is: (1) measure the impedance of the piezoelectric layer over the frequency range of f_i to f_f within the range of $f_i < f_n < f_f$, where f_i, f_n, and f_f are the initial, resonant, and final frequencies, (2) record the maximum frequency (i.e., the resonant frequency) and the time, (3) plot the resonant frequency versus the time, (4) repeat Steps 1, 2, and 3, and (5) stop program.

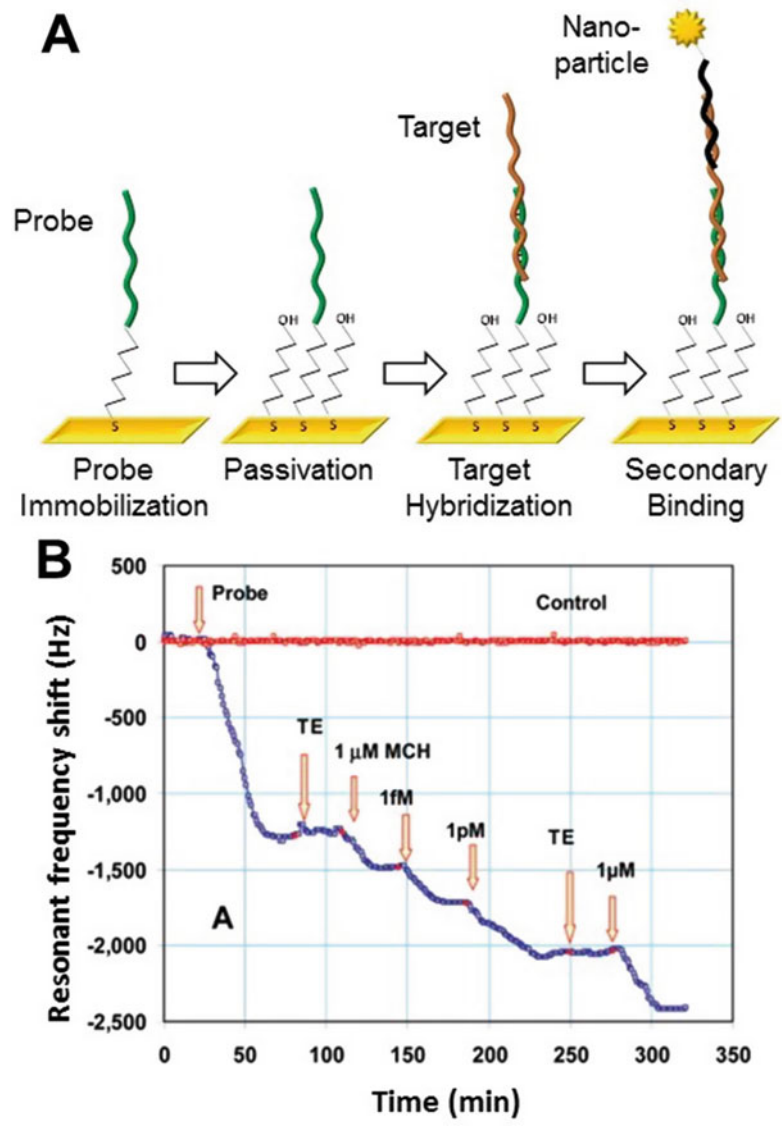

Fig. 4 (**a**) Schematic of the sequential binding steps in detection of DNA and RNA including probe immobilization, surface passivation, target hybridization, and response verification (here the secondary binding of DNA-functionalized AuNPs). Reproduced from Johnson and Mutharasan with permission from the American Chemical Society [9]. (**b**) Representative sensor response for real-time DNA sensing in continuously flowing liquid showing DNA probe immobilization (*t*~25 min.), buffer rinse (*t*~75 min.), surface passivation with MCH (*t*~110 min.), detection of a 1 fM target sample (*t*~150 min.), detection of a 1 pM target sample (*t*~190 min.), buffer rinse (*t*~250 min.), and sensor saturation with a 1 μM target sample (*t*~280 min.). Reproduced from Rijal and Mutharasan with permission from the American Chemical Society [12]

5. The sensor is first installed and allowed to reach steady state in a continuously flowing buffer.
6. After the resonant frequency reached steady state, the most dilute reduced probe solution is added to the recirculating buffer at a typical flow rate of 200–1000 μL/min to immobilize the DNA probe on the sensor Au surface.
7. After the sensor response reached steady state, another addition of DNA-containing solution is made, but at a higher concentration. As shown in Fig. 4b, this process can be repeated until the Au surface is saturated with DNA probe (*see* **Note 6**).
8. Following deposition of the DNA probe, the flow is returned to buffer in a single pass mode to remove any unbound DNA from the system.

3.6 Surface Passivation

1. After the system is flushed, the unoccupied Au <111> sites are filled by adding 1 mL of MCH (730 μM) to the flow loop and placing the flow in a recirculation mode.
2. After the sensor response reached steady state, the flow loop is flushed with buffer to remove any unbound MCH from the system (*see* **Notes 7** and **8**).

3.7 Target Hybridization

1. The stock target sample is first used to create serial dilutions in buffer ranging from nanomolar (nM) to attomolar (aM) levels. Detailed procedures for extraction and preparation of DNA and RNA are provided in our previous studies [10, 11]. Synthetic DNA and RNA targets as short as 10–30 bases, [9, 12] as well as relatively longer strands derived from biological samples have been detected [10, 11].
2. Following DNA probe immobilization and backfilling, the flow is changed to the most dilute target-containing sample and is placed in a recirculation mode.
3. As shown in Fig. 5a, the sensor response is then continuously monitored as target hybridization occurred. Note the typical exponential characteristic of the sensor response during hybridization of the target strand.
4. After the sensor response reached steady state, another addition of target-containing sample is made, but at a higher concentration. Similar to the immobilization of the DNA probe, this process can be repeated until the immobilized DNA probes become saturated with hybridized target strands. The technique of cyclic hybridization also adds confidence to the measurement as it provides an internal control and enables the evaluation of the limit of detection (LOD).
5. After the sensor response reaches steady state, the flow is returned to buffer in a single pass mode to remove any unbound DNA from the system.

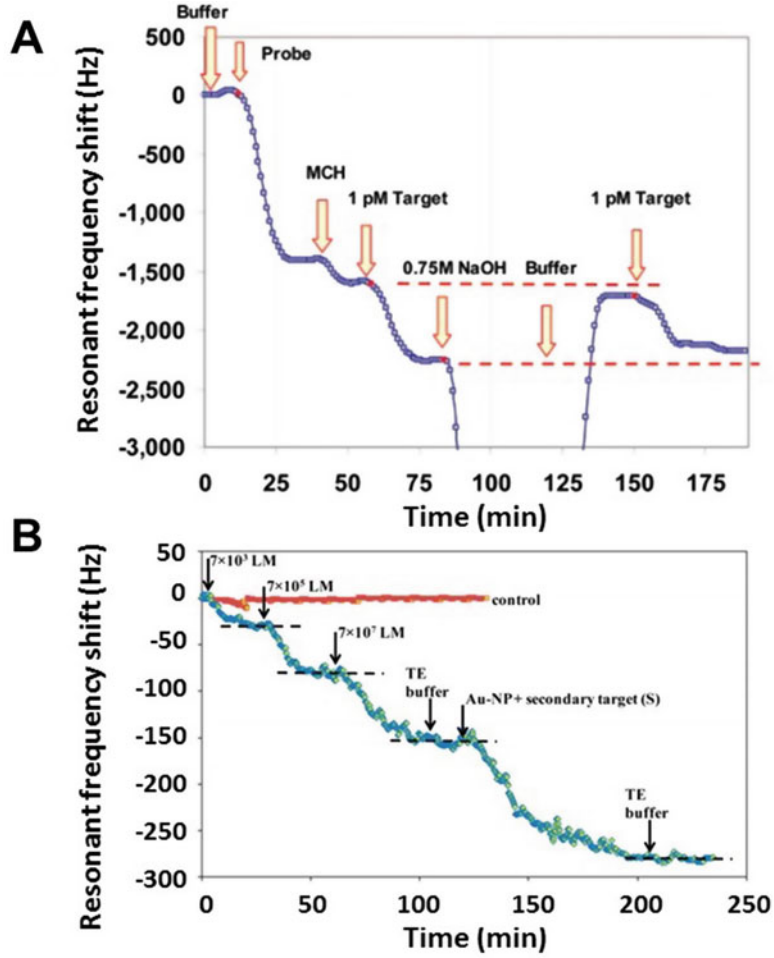

Fig. 5 (**a**) Real-time sensing of DNA hybridization (*t* ~50 min.) followed by subsequent in situ dehybridization (*t* ~90 min.) and rehybridization (*t* ~150 min). Reproduced from Rijal and Mutharasan with permission from the American Chemical Society [12]. (**b**) Sensor response amplification by secondary binding of DNA-functionalized AuNPs (*t* ~125 min.). Reproduced from Sharma and Mutharasan with permission from the American Chemical Society [10]

3.8 Secondary Binding

1. AuNPs are functionalized by mixing 100 μL of stock AuNP solution with 300 μL of 3 μM secondary DNA probe and 1 μL of stock TCEP.
2. After 1 h, the AuNPs are then washed by repeated centrifugation and resuspended in 1 mL buffer.
3. As shown in Fig. 5b, the addition of DNA-functionalized AuNPs to the flow loop causes a further decrease in the resonant frequency in the presence of the hybridized target species (*see* **Note 9**).

3.9 Reversible Binding

1. To dehybridize the target strand and regenerate the sensor surface, the flow is switched to a NaOH solution in a single pass mode (*see* Fig. 5a; *see* **Note 10**). Following dehybridization, the flow may then be returned to buffer and a new target strand rehybridized as shown in Fig. 5a. The process of cyclic hybridization and dehybridization also adds confidence to the measurement as it provides an internal control and enables high-throughput analysis.

4 Notes

1. *Micro-soldering Conditions*—Given PEMC sensors transduce target hybridization in terms of change in the resonant frequency which is measured through the piezoelectric layer, the means by which the electrical leads are bonded to the piezoelectric layer prior to anchoring are important fabrication considerations. Various micro-soldering strategies are available which provide controlled soldering temperature and solder deposition.
2. *Flexibility in Electrical Insulation*—Given the insulating polymers are applied via spin coating and chemical vapor deposition, it is possible to use alternative polymers to insulate the PZT layer. For example, hydrophobic coatings, such as SU-8, have been applied [24].
3. *Cleaning Sensor Surfaces using Piranha Solution*—Warning: Piranha solution is highly corrosive and should be handled with care. Overexposure of the sensor to piranha solution should be avoided and can result in film peeling and surface pitting effects [25].
4. *Disulfide Reduction using TCEP*—It should be noted that alternative strategies for reduction of the disulfide bond are also available [12].
5. *Bio-conjugation Techniques for Detection of Proteins, Toxins, Viruses, and Cells*—In addition to functionalizing the surface for detection of DNA and RNA, various bio-conjugation strategies may be employed for detection of proteins, toxins, viruses, and cells. For example, approaches based on protein G adsorption and silanization have been used for the immobilization of antibodies in antibody-based PEMC sensing applications. Collectively, thiolated self-assembled monolayers, [26] protein G, [27] carbodiimide-based crosslinking (e.g., 1-ethyl-3-(3-dimethylaminopropyl)carbodiimide (EDC)), [28] and silanization (e.g., (3-aminopropyl)triethoxysilane (APTES)) [28, 29] approaches enable the application of PEMC sensors for detection of a wide range of targets including DNA and RNA as well as proteins, toxins, viruses, and cells [7].

6. *Concentration-dependent Binding Responses and Internal Controls*—In all experiments, returning the flow to buffer after target hybridization caused no shift in the resonant frequency indicating that the target strand remained hybridized and verifying that the sensor response is indeed due to target hybridization and is not the result of a fluid density or viscosity effect. We also note that no net change in the sensor response is observed when target-free samples are added to the system. Analysis of concentration-dependent hybridization responses also provides sensitivity data for sensor characterization and an internal control for sensor response.
7. *Vibration-induced Surface Passivation*—It has recently been shown that acoustic forces generated by ultrasonic vibration in micro-electromechanical systems (MEMS) may contribute to a reduction in the level of nonspecific binding to the sensor [30, 31]. Thus, in addition to the high cantilever Reynolds number which enables continuous measurement in liquid, the ability to passivate the surface using both surfactant- and acoustic-based techniques supports selective biosensing in complex matrices.
8. *Considerations of Secondary Binding Agent*—When designing a secondary binding assay, two important considerations arise as a result of the added mass-based sensing principle: (1) the binding strength between the secondary binding species and the target, and (2) the added mass contribution of the secondary binding species. Efforts should be taken to optimize both aspects when designing an effective secondary binding assay. We also note that secondary binding increases the net sensor response per target molecule which both increases the LOD and improves the confidence of the measurement, as the secondary hybridization event is designed to only occur if the target strand is hybridized to the immobilized probe.
9. *Reversible Binding*—Efforts should be taken to examine cyclic hybridization and dehybridization as an internal control and to increase the measurement throughput. It is also of interest to determine the effect of the sensor regeneration on the biorecognition layer by examining signal hysteresis.
10. *Use of Complementary Transduction Mechanisms*—It has been demonstrated that the use of dual transduction mechanisms, such as the use of an electrochemically active sensing area, can also provide complementary information on the target hybridization event, making the measurement highly robust [32].

References

1. Chen X, Zhang JF, Zen K, Zhang CY (2011) MicroRNAs as blood-based biomarkers of cancer. MicroRNAs in cancer translational research. Springer, New York
2. Mitchell PS, Parkin RK, Kroh EM, Fritz BR, Wyman SK, Pogosova-Agadjanyan EL, Peterson A, Noteboom J, O'Briant KC, Allen A, Lin DW, Urban N, Drescher CW, Knudsen BS, Stirewalt DL, Gentleman R, Vessella RL, Nelson PS, Martin DB, Tewari M (2008) Circulating microRNAs as stable blood-based markers for cancer detection. P Natl Acad Sci USA 105:10513–10518
3. Mostert B, Sieuwerts AM, Martens JWM, Sleijfer S (2011) Diagnostic applications of cell-free and circulating tumor cell-associated miRNAs in cancer patients. Expert Rev Mol Diagn 11:259–275
4. Yu DC, Li QG, Ding XW, Ding YT (2011) Circulating microRNAs: potential biomarkers for cancer. Int J Mol Sci 12:2055–2063
5. Sharma H, Mutharasan R (2013) Review of biosensors for foodborne pathogens and toxins. Sens Actuators B 183:535–549
6. McKillip JL, Drake M (2004) Real-time nucleic acid-based detection methods for pathogenic bacteria in food. J Food Prot 67:823–832
7. Johnson BN, Mutharasan R (2012) Biosensing applications using dynamic-mode cantilever sensors: a review. Biosens Bioelectron 32:1–18
8. Johnson BN, Mutharasan R (2014) Biosensor-based microRNA detection: techniques, design, performance, and challenges. Analyst 139:1576–1588
9. Johnson BN, Mutharasan R (2012) Sample preparation-free, real-time detection of microRNA in human serum using piezoelectric cantilever biosensors at attomole level. Anal Chem 84:10426–10436
10. Sharma H, Mutharasan R (2013) hlyA gene-based sensitive detection of *Listeria monocytogenes* using a novel cantilever sensor. Anal Chem 85:3222–3228
11. Johnson BN, Mutharasan R (2013) A cantilever biosensor-based assay for toxin-producing cyanobacteria *Microcystis aeruginosa* using 16S rRNA. Environ Sci Technol 47:12333–12341
12. Rijal K, Mutharasan R (2007) PEMC-based method of measuring DNA hybridization at femtomolar concentration directly in human serum and in the presence of copious noncomplementary strands. Anal Chem 79:7392–7400
13. Johnson BN, Mutharasan R (2011) Persistence of bending and torsional modes in piezoelectric-excited millimeter-sized cantilever (PEMC) sensors in viscous liquids-1 to 10 (3) cP. J Appl Phys 109:066105
14. Timoshenko S (1937) Vibration problems in engineering, Second edn. Van Nostrand Company, Inc., New York, NY
15. Maraldo D, Mutharasan R (2010) Mass-change sensitivity of high-order mode of piezoelectric-excited millimeter-sized cantilever (PEMC) sensors: Theory and experiments. Sens Actuators B 143:731–739
16. Johnson BN, Mutharasan R (2011) A novel experimental technique for determining node location in resonant mode cantilevers. J Micromech Microeng 21:065027
17. Ziegler C (2004) Cantilever-based biosensors. Anal Bioanal Chem 379:946–959
18. Sader JE (1998) Frequency response of cantilever beams immersed in viscous fluids with applications to the atomic force microscope. J Appl Phys 84:64–76
19. Johnson BN, Sharma H, Mutharasan R (2013) Torsional and lateral resonant modes of cantilevers as biosensors: alternatives to bending modes. Anal Chem 85:1760–1766
20. Johnson BN, Mutharasan R (2011) The origin of low-order and high-order impedance-coupled resonant modes in piezoelectric-excited millimeter-sized cantilever (PEMC) sensors: experiments and finite element models. Sens Actuators B 155:868–877
21. Sharma H, Lakshmanan RS, Johnson BN, Mutharasan R (2011) Piezoelectric cantilever sensors with asymmetric anchor exhibit picogram sensitivity in liquids. Sens Actuators B 153:64–70
22. Johnson BN, Mutharasan R (2010) Expression of picogram sensitive bending modes in piezoelectric cantilever sensors with nonuniform electric fields generated by asymmetric electrodes. Rev Sci Instrum 81:125108
23. Van Eysden CA, Sader JE (2006) Resonant frequencies of a rectangular cantilever beam immersed in a fluid. J Appl Phys 100:114916
24. Rijal K, Mutharasan R (2007) Method for measuring the self-assembly of alkanethiols on gold at femtomolar concentrations. Langmuir 23:6856–6863
25. Johnson BN, Mutharasan R (2013) Regeneration of gold surfaces covered by adsorbed thiols and proteins using liquid-phase hydrogen peroxide-mediated UV-Photooxidation. J Phys Chem C 117:1335–1341
26. Campbell GA, Mutharasan R (2005) Monitoring of the self-assembled monolayer of 1-

hexadecanethiol on a gold surface at nanomolar concentration using a piezo-excited millimeter-sized cantilever sensor. Langmuir 21:11568–11573

27. Johnson BN, Mutharasan R (2012) pH effect on protein G orientation on gold surfaces and characterization of adsorption thermodynamics. Langmuir 28:6928–6934
28. Campbell GA, Delesdernier D, Mutharasan R (2007) Detection of airborne *Bacillus anthracis* spores by an integrated system of an air sampler and a cantilever immunosensor. Sens Actuators B 127:376–382
29. Campbell GA, Mutharasan R (2008) Near real-time detection of *Cryptosporidium parvum* oocyst by IgM-functionalized piezoelectric-excited millimeter-sized cantilever biosensor. Biosens Bioelectron 23:1039–1045
30. Johnson BN, Mutharasan R (2014) Reduction of nonspecific protein adsorption on cantilever biosensors caused by transverse resonant mode vibration. Analyst 139:1112–1120
31. Meyer GD, Moran-Mirabal JM, Branch DW, Craighead HG (2006) Nonspecific binding removal from protein microarrays using thickness shear mode resonators. Sensors 6:254–261
32. Johnson BN, Mutharasan R (2013) Electrochemical piezoelectric-excited millimeter-sized cantilever (ePEMC) for simultaneous dual transduction biosensing. Analyst 138:6365–6371
33. Maraldo D, Rijal K, Campbell G, Mutharasan R (2007) Method for label-free detection of femtogram quantities of biologics in flowing liquid samples. Anal Chem 79:2762–2770